Probing Protein Folding and Conformational Transitions with Fluorescence

Catherine A. Royer

Centre de Biochimie Structurale, 29, rue de Navacelles 34090 Montpellier Cedex France

Received October 5, 2004

Contents

Catherine Royer received her License in Chemistry and Biochemistry from the University of Pierre and Marie Curie, Paris 6, in 1979 and her Ph.D. in Biochemistry from the University of Illinois at Urbana-Champaign in 1985. She was awarded an NSF–CNRS and a CNRS postdoctoral fellowship to work at the University of Paris and the CNRS from 1985 to 1987 under the direction of Bernard Alpert and Guy Hervé. From 1987 to 1990 she served as User Coordinator of the Laboratory for Fluorescence Dynamics in the Department of Physics and as Adjunct Assistant Professor of Biochemistry at the University of Illinois. In 1990 she joined the faculty as Assistant Professor of Pharmaceutics in the School of Pharmacy at the University of Wisconsin—Madison, and she was promoted to Associate Professor with tenure in 1995. In 1997 she became the Director of Research at the Center for Structural Biochemistry of INSERM and CNRS in Montpellier France, and she is currently the Associate Director of the Center. In 2000 she was elected as a Fellow of the American Association for the Advancement of Science. Her research interests include fluorescence spectroscopy as applied to protein folding, the effects of pressure on protein stability, and the physical basis for the regulation of gene expression.

1. Introduction

Fluorescence arguably constitutes the most widely used experimental approach in the field of protein folding. Hence, any review of the use of fluorescence to probe protein stability and conformational dynamics is necessarily incomplete with respect to the current and past literature. Rather than a review of the literature, I will attempt to present specific examples of a variety of fluorescence experimental approaches, both classical and novel, to the study of protein folding, with a discussion of the advantages and limitations of each.

In general, the reason fluorescence has been so widely applied to studies of protein folding and protein conformational dynamics stems from three fundamental properties of this technique. First, fluorescence signals are exquisitely sensitive to the immediate environment of the probe, which, under appropriate circumstances (discussed below), changes drastically upon unfolding. Second, the technique provides a very high signal-to-noise ratio using relatively small amounts of material. The high sensitivity of the fluorescence signal (as low as pM for certain dyes) is particularly useful for in-depth thermodynamic studies involving multiple experiments under different conditions (solvent, temperature, pressure, ligand, etc.), because it limits significantly the amount of material required. It is also useful in ϕ-value studies, since the use of fluorescence precludes the need to produce large quantities of the mutant proteins.[1−6] Third, in addition to the high detection sensitivity of fluorescence, the time scale of emission is in the nanosecond range. This, coupled with the high signal-to-noise ratio, allows for data acquisition times to be quite fast relative to the time scales for the folding and conformational transitions. Thus, the experiments are not limited in time resolution by the need to signal average. Finally, in addition to its obvious advantages in kinetics experiments, the rapid data acquisition in fluorescence is also appreciable (which makes it generally the method of choice) in the type of in-depth studies mentioned above, simply because the experiments take much less time.

Despite these clear advantages of fluorescence with respect to other commonly used techniques in the field of protein folding, a number of limitations must be recognized as well. Most generally, fluorescence is a local signal. The fluorescence observable in most traditional experiments reports on the environment directly surrounding the probe. This limits and complicates the interpretation of the changes in the fluorescence signal in terms of their structural origin. Typically, the information one can obtain directly from the interpretation of the fluorescence parameters is limited to the degree of exposure of the fluorophore to the solvent and the extent of its local mobility. In folding studies, it is necessary to compare the observed fluorescence changes with

10.1021/cr0404390 CCC: $59.00
Published on Web 04/25/2006

changes in the circular dichroism, FTIR, or, when possible, NMR spectrum of the protein. This allows one to ascertain the extent to which the modifications in the local environment of the fluorescent probe upon folding or unfolding correlate with changes in the secondary structure of the protein. Typically, fluorescence is not used directly to infer detailed structural information about intermediates or pathways in folding. Rather, the thermodynamic and kinetic parameters obtained from the fluorescence profiles are themselves interpreted on a structural level. Two notable exceptions to the local character of the fluorescence signal are Förster resonance energy transfer (FRET) experiments and fluorescence correlation spectroscopy (FCS) experiments, which will be discussed in detail below.

2. Intrinsic Protein Fluorescence

Most proteins contain amino acid residues that are intrinsically fluorescent: tryptophan, tyrosine, and phenylalanine. Tryptophan is by far the most useful of the three. Although large changes in protein conformation clearly modify the intensity of tyrosine and phenylalanine fluorescence, as well as the local mobility of these side chains as assessed by anisotropy measurements, their low extinction coefficients and quantum yields, coupled with the relative lack of environmental sensitivity of their emission energy, render them significantly less useful than tryptophan. This actually can be an advantage because proteins tend to contain fewer tryptophan residues than tyrosine and phenylalanine, and therefore, more specific local information can be attained by selectively exciting the tryptophan residues using excitation wavelengths of 295 nm or above. I will limit the discussion of folding using intrinsic protein fluorescence to studies involving observation of the changes in the fluorescence of tryptophan residues.

Tryptophan, due to its aromatic character, is often (although not always) found fully or partially buried in the hydrophobic core of protein interiors, at the interface between two protein domains or subdomains, or at the subunit interface in oligomeric protein systems. Upon disruption of the protein's tertiary or quaternary structure, these side chains become more exposed to solvent. Since the excited-state dipole moment of tryptophan is quite large (~6 D),[7] the emission energy is highly sensitive to the polarity (and dynamics) of the environment. Those residues that are fully or partially buried in the relatively hydrophobic interior or interfaces of proteins will exhibit blue-shifted emission anywhere from 309 nm in the azurin protein interior[8] to more typical 335 nm[9] in a partially buried configuration. The spectra of tryptophan in folded proteins are clearly identifiable relative to the spectrum of tryptophan when it is exposed to water with a maximum at 355 nm. In Figure 1 is shown the structure of an activated mutant of the bacterial antiterminator LicT.[10] The unique tryptophan residue in the protein is exposed to solvent in the wild type (WT), whereas, in a mutant that mimics the phosphorylated form of the protein (Figure 1a), the tryptophan, shown in purple, is partially buried at the interface between two domains. One can see from the spectra in Figure 1b that the emission of the mutant forms (H207D/H269D) is shifted significantly to the blue (~335 nm) with respect to the case of the wild type (LicT-WT and LicT-PRD), the maximum of which, near 355 nm, corresponds to the spectrum of tryptophan in water. These observations were used (with others) to propose that activation of this protein by phosphorylation leads to the burial of the tryptophan residues by rotating a hinge between the two subdomains.

While the emission energy of even a partially buried tryptophan residue in a folded protein will invariably shift to the red upon unfolding, it is not possible to predict what the effect of solvent exposure will be upon the quantum yield (total intensity) of emission. This is due to the fact that the quantum yield of tryptophan in proteins is difficult to predict. Several amino acid side chains, as well as the peptide bond, are efficient quenchers of tryptophan fluorescence through excited-state proton or electron transfer.[11,12] Indeed the three major lifetime values near 5, 2, and 0.5 ns observed for most tryptophan residues in proteins have been proposed to arise from differential quenching probabilities of the peptide bond for the three major side chain $\chi 1$ rotamers,[11−16] although decay heterogeneity can also arise from solvent or protein matrix relaxation around the excited state. The values and importance of these three decay times for any given tryptophan residue are further modified by the immediate environment, which can constrain certain rotamer populations or present particular quenching groups. If no major quenching or energy transfer to prosthetic groups (heme groups, NADH, or other trypophan residues) occurs in the folded state, then one can predict that solvent quenching resulting from tryptophan exposure upon unfolding will lead to an overall decrease in the intensity of emission, such as in the case of the small β-barrel protein, $P13^{MTCP1}$ (Figure 2).[17] However, in cases where strong quenching occurs in the folded structure, exposure to solvent may actually result in an increase in overall fluorescence intensity (see the case of trp99 in the *trp* repressor in Figure 7B).[18] Thus, when carrying out the first fluorescence-based unfolding study of any protein, it is best to record the entire spectrum as a function of the perturbation (denaturant, temperature, pressure, ...). In subsequent studies, particularly in kinetics studies which require fast data acquisition, typically one sets the emission monochromator at a single wavelength, preferably one at which either a large increase or a large decrease in fluorescence intensity is observed, and then the intensity is recorded as a function of time after the perturbation (as an example, see ref 19). Note that the direction of the signal change depends on the wavelength of observation. For example, due to the red-shift upon unfolding of P13 (Figure 2), the intensity decreases at 320 nm upon unfolding, whereas, at 400 nm, an increase in intensity is observed.[17] Clearly, one should avoid the isobestic point at ~370 nm.

2.1. Proteins without Tryptophan

Depending upon the protein in question, one may chose a variety of different strategies to apply to fluorescence-based folding studies. A few proteins do not contain any tryptophan residues. The best approach in this case is to substitute a tryptophan residue in place of a tyrosine residue. The circular dichroism and (when possible) the HSQC spectra of the WT and mutant proteins should be compared, as well as their CD-based unfolding profiles in order to ensure that the substitution has not modified significantly the structure, stability, and folding properties of the protein. This approach has been quite successful in the case of the IgG binding domain of protein L from *Peptostreptococcus magnus*.[20] Figure 3 shows the folded and unfolded state spectra of the WT protein L (containing several tryrosine residues) and that of a mutant protein L in which tyrosine 43 was substituted by tryptophan. Also apparent in Figure 3 is the remarkable

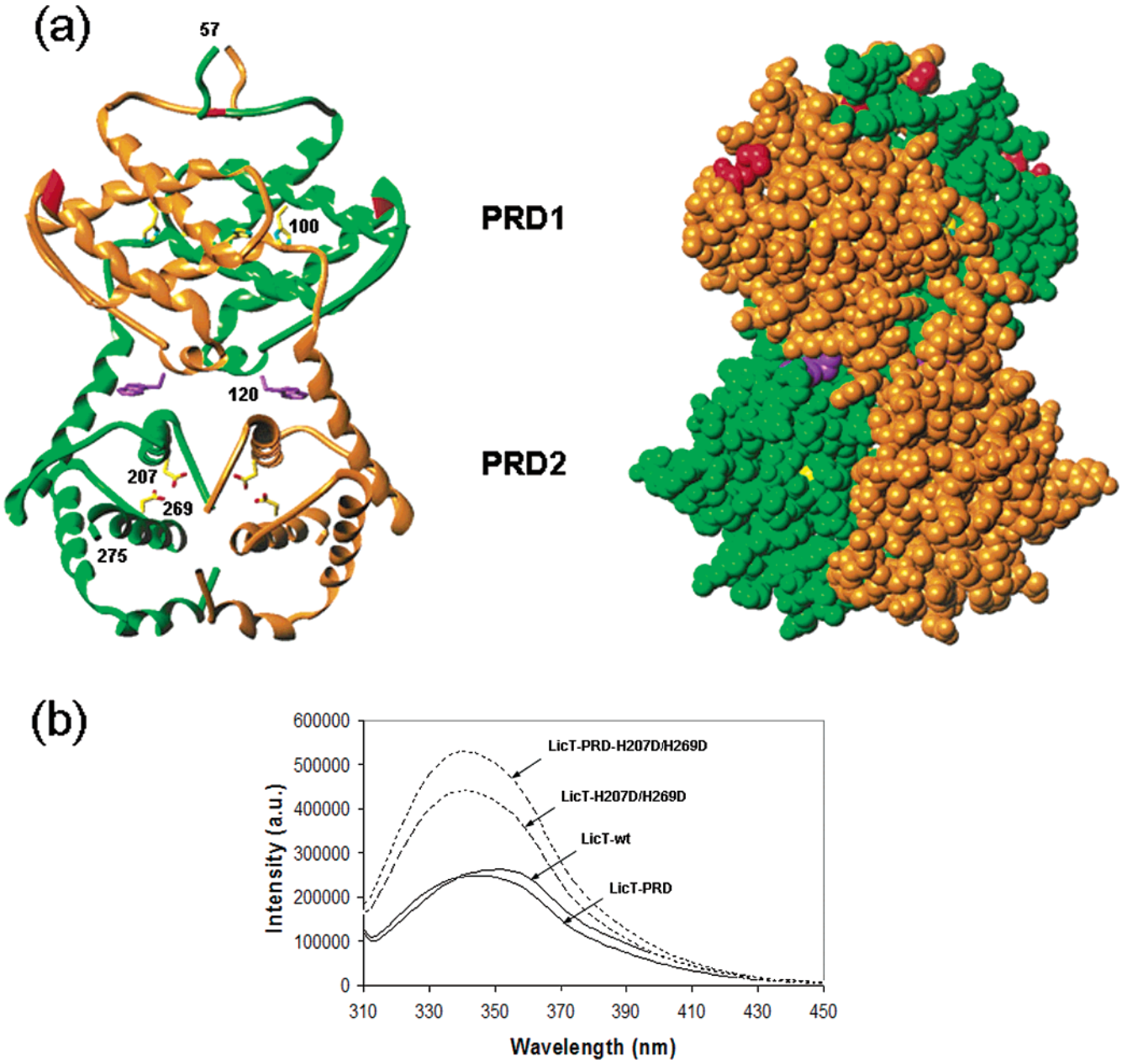

Figure 1. (a) Structure of the regulatory domains of an activated mutant of LicT (tryptophan residues are in purple); (b) intrinsic fluorescence emission spectra of the WT and activated mutant forms. (Reprinted with permission from ref 10. Copyright 2001 Elsevier.)

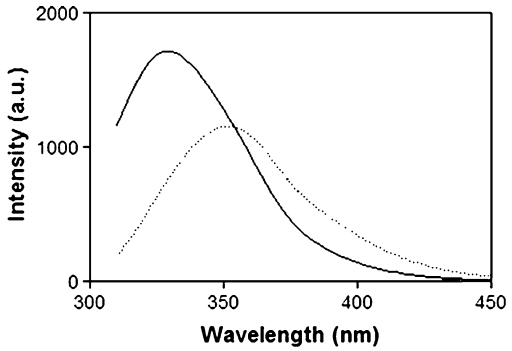

Figure 2. Intrinsic tryptophan emission of $P13^{MTCP1}$ in buffer (full line) and 3 M guanidine hydrochloride (dotted line). (Reprinted with permission from ref 17. Copyright 2001 Elsevier.)

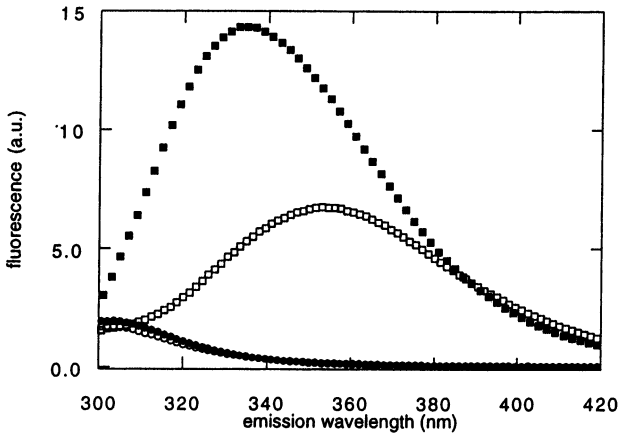

Figure 3. Intrinsic emission spectra of WT protein L (circles) and the Y43W mutant (squares) under native (closed symbols) and denaturing (open symbols) conditions. (Reprinted with permission from ref 20. Copyright 1997 American Chemical Society.)

difference in total fluorescence emission (alluded to above) between (several) tyrosines and the one tryptophan, in addition to the much more significant changes observed upon

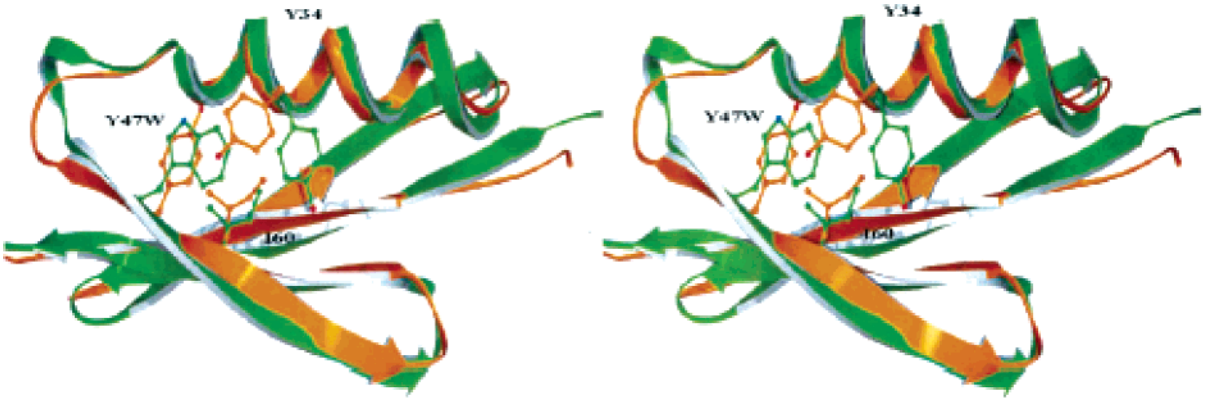

Figure 4. Stereoview of ribbon model overlays of the WT* form (green) and the WT NMR-derived solution #1 model (orange). The proteins exhibit the same overall fold, although the main-chain rmsd is 1.46. Major differences occur in the loop regions as well as the N-terminus of β-strand 4. The side chains for residues Y47/W47, Y34, and I60 are shown. (Reprinted with permission from ref 96 (http://journals.iucr.org/). Copyright 2001 The International Union of Crystallographers.)

unfolding for the tryptophan containing protein. Not only did the Baker group compare the CD and NMR properties of the WT and trp substituted proteins, but they went on to determine the crystal structure of the mutant protein (Figure 4), which exhibited some packing differences in the core compared to the WT structure. Fortunately, the Y → W substitution made little difference to the overall stability and unfolding properties of the protein. Baker's group has used this mutant protein L in a significant series of studies probing the fundamental principles of protein folding.[20−26] In particular, these authors have examined the relationships between sequence and stability, the nature of the transition state, the role of entropy and topology in defining the folding parameters, and the fundamental thermodynamics that control the folding of this protein.

Another approach is to use tryptophan scanning mutagenesis to place single tryptophan residues at various positions in the protein as a means of probing the local unfolding in different domains or subdomains. One should be aware, however, that the replacement of an amino acid by tryptophan can lead to changes in the stability[27] and even in the cooperativity of unfolding. Thus, relatively complete structural and thermodynamic analyses of each of the tryptophan substitution mutants is required, and even so, the comparisons between folding domains that one can make from such studies are often limited by the perturbations brought about by the mutations.

2.2. Single Tryptophan Proteins

Some proteins contain a unique tryptophan residue. In this case, information about the solvent exposure of this unique tryptophan, and thus the structural integrity of the surrounding environment, can be obtained directly. Staphylococcal nuclease (Snase) (Figure 5) is one such protein. Since the pioneering work of Anfinsen,[28] this protein has served as a model for a large number of folding studies, about half of which have been based on the changes in the fluorescence of its single tryptophan residue. Interestingly, this residue at position 140 is the last to be ordered in the crystal structure,[29] yet it exhibits almost no local rotational motion in the native state, and its emission spectrum, with a maximum near 335 nm, corresponds to that of a fairly buried tryptophan. Tryptophan 140 in Snase is also, along with serine 141, key to the formation of a compact, folded native structure,[30,31] an observation which highlights the recurrent role of tryptophan in providing protein structural stability.

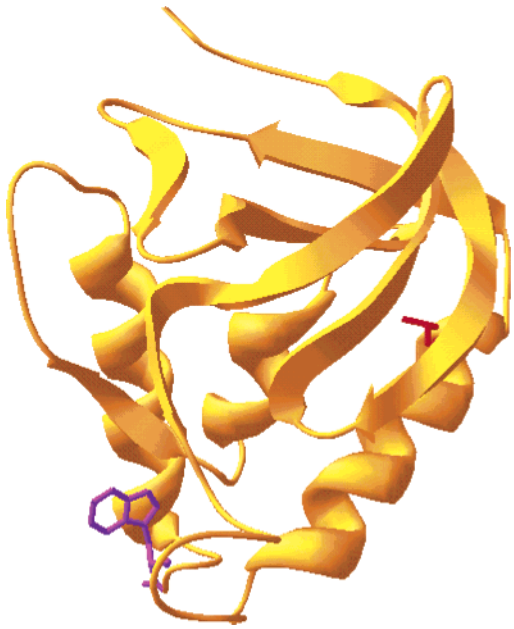

Figure 5. Ribbon representation of the 3-D structure of nuclease.[29] Note that the tryptophan residue (purple) is the last residue in the sequence that exhibits order.

Thus, as in many cases, the unfolding of Snase can be studied by fluorescence intensity, emission energy, and/or anisotropy if care is taken to factor in the changes in quantum yield for the latter two observables.[32] The advantage of single tryptophan containing proteins is that one need not attempt to assign the fluorescence signal and any observed changes in that signal upon unfolding to the different tryptophan residues in the protein. However, a distinct disadvantage resides in the fact that a single tryptophan residue provides information about the structural integrity of its immediate environment. For single tryptophan proteins containing multiple domains or subdomains, or which populate partially folded intermediates, the fluorescence signal often fails to report on these phenomena if they involve regions of the protein that are distant from the single tryptophan. Thus, if one seeks information concerning other regions of the protein, the unique tryptophan can be substituted, preferably by tyrosine, in order to preserve to the extent possible the WT stability and folding properties, and another tryptophan can be placed at alternative positions in the structure. A recent study of Snase using this approach[33] revealed an early folding

intermediate involving the β-barrel region of the protein. It is important, as was done in this study, to verify, using alternative techniques, that the same intermediate forms in the WT protein and is not the result of the mutation.

2.3. Multiple Trytpophan Containing Proteins

Most commonly, one is confronted with proteins containing two or more tryptophan residues. This situation can be considered both advantageous and limiting. With tryptophan residues distributed throughout the 3-D structure, non-2-state folding behavior is more readily detected. Assigning particular phases of the transitions to specific tryptophan residues, and thus to specific domains or regions of the structure, is often possible. One approach is to carry out emission wavelength-dependent studies of the fluorescence decay as a function of denaturant concentration. These experiments can be referred to as unfolding DAS, or UDAS, where DAS refers to decay associated spectra.[34,35] Although each tryptophan typically will exhibit at least two, and often more, decay times or lifetimes (generally around 5, 2, and 0.5 ns), it is also true that in proteins the contributions of these individual decay rates to the overall decay of each tryptophan are often very different. Hence, although one cannot assign each of the DAS to an individual tryptophan residue, if there are only two or three tryptophan residues in the protein, each of the DAS is often dominated by contributions from only one of them. Usually, to unequivocally assign the unfolding phases to individual tryptophan residues, one needs to substitute the tryptophan residues by mutagenesis (typically by tyrosine or phenylalanine to minimize the perturbations), leaving only one at a time, and carry out the unfolding studies of each mutant. The first such study was carried out on the *trp* repressor dimer unfolding transition.[18,36,37]

The *trp* repressor contains two tryptophan residues per monomer (Figure 6). Trp 19 (blue) was shown to be quite

Figure 6. Ribbon diagram of the crystal structure of the *trp* repressor.[98] The tryptophan 19 side chains from both subunits are red, and those corresponding to tryptophan 99 e are blue.

blue-shifted and to exhibit decay components of near 4−5 and 2 ns, whereas the fluorescence of trp 99 (red) is much redder and is dominated by the short 0.5 ns component. The WT type fluorescence is very close to a weighted sum of the decays of the two mutants. Upon unfolding, the WT protein's fluorescence emission shifts to the red and the intensity increases. For the WT and the mutant proteins, the fluorescence decay was measured at multiple emission wavelengths and at each concentration of denaturant. Then the DAS were calculated from the fractional intensities of the decays and the total fluorescence spectrum.[35] The steady-state studies of the single trp mutants revealed that the red-shift observed for the WT protein was due primarily to the exposure of tryptophan 19 to solvent (Figure 7A), whereas the intensity

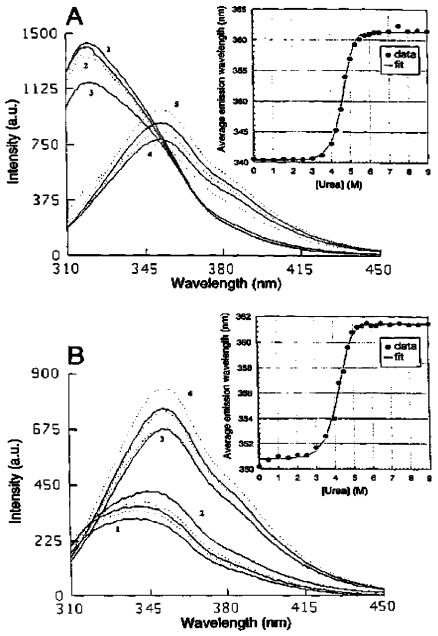

Figure 7. Steady-state spectra as a function of urea concentration for (A) trpR W99F and (B) W19F mutants. Increasing numbers correspond to increasing urea concentration. Insets: Urea unfolding profiles based on the average emission wavelength. (Reprinted with permission from ref 18. Copyright 1993 The Protein Society.)

increase arose from the dequenching of residue 99, which was highly quenched in the folded state (Figure 7B).

The evolution of the DAS for the two mutant proteins as a function of urea concentration reveals that the emission from trp 19 (Figure 8A) is almost entirely due to a component at 4.25 ns, that is highly blue-shifted in the native state but which shifts red and loses total intensity as the protein unfolds, whereas the fractional contribution of the 0.75 ns component increases with increasing urea. In the case of trp 99, the fluorescence of the folded state is dominated by a short component at 0.57 ns, whose contribution decreases in favor of components at 5 and 2.4 ns (Figure 8B) as the protein unfolds. The proteins that I have studied to date in terms of the dependence of the fluorescence decay upon denaturant concentration exhibit this type of behavior.[17,38] Indeed, the values of the lifetime components do not change significantly upon unfolding. Rather, their fractional contributions are dependent upon the denaturant concentration. This is not an artifact of the global analysis of the data, since the results are nearly identical in single curve analyses. And in fact, the three typical components near 0.5, 2, and 5 ns are those observed for unstructured tryptophan containing peptides.

These observations of the dependence upon unfolding of the time-resolved fluorescence properties of tryptophan in proteins provide support for the notion that while dynamics surely contributes to some extent, to the heterogeneity of tryptophan emission, the fundamental basis for the three observed lifetimes lies in the population of the three rotamers around the Cα−Cβ bond.[11−14,16,39] Indeed, the fractional populations (as opposed to fractional intensities) of the three lifetimes are often close to equivalent (~33%) in unfolded proteins and unstructured peptides, consistent with similar relative energies and thus equal population of the three rotamers in the absence of secondary and tertiary structure.

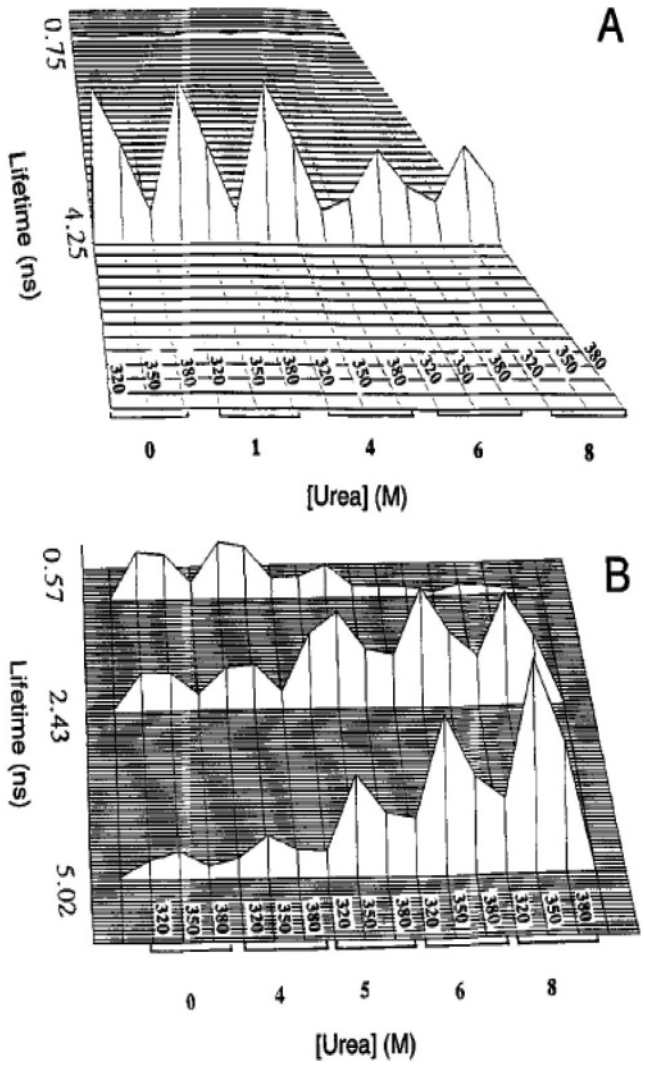

Figure 8. DAS as a function of urea concentration for (A) trpR W99F and (B) W19F mutants. Increasing numbers correspond to increasing urea concentration. (Reprinted with permission from ref 18. Copyright 1993 The Protein Society.)

3. Extrinsic Dyes

3.1. Folding Intermediates Studied with ANS

In 1954, Weber and Laurence[40] published a study in which they demonstrated that the quantum yield of 1-anilinophthalene-8-sulfonic acid (ANS) in water (0.004) increased enormously (to 0.75) when bound to bovine serum albumin (BSA). Weber went on in 1963 to use this property of ANS to investigate the origin of the acid expansion of BSA.[41] Hence, Weber was the first to use this probe to monitor the acid-induced unfolding of a protein. Later, Stryer[42] showed that ANS would bind to the heme pockets of apomyoglobin and apohemoglobin. Turner and Brand[43] provided a quantitative estimation of the polarity of different protein binding sites for several arylaminonaphthalene sulfonates by measuring the emission energy of the bound probes. Since these early experiments, ANS has been copiously used to identify equilibrium and kinetic intermediates in protein folding studies. While ANS has proven quite useful in the characterization of the populated intermediates in protein folding, the structural information that can be gleaned from such studies is often rather vague and must be complemented by data from circular dichroism, NMR, FTIR, or other structural techniques. Another example of the use of ANS to identify folding intermediates can be found in the study by Goto and Fink[44] on the high salt acid and alkaline denatured states of β-lactamase. Both the large increase in quantum yield of ANS and the significant blue-shift upon protein binding previously reported are apparent in the spectra in Figure 9.

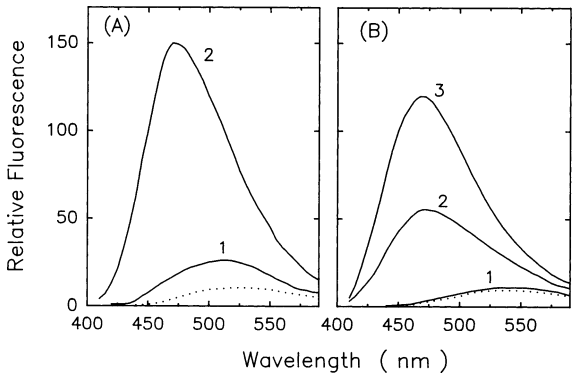

Figure 9. Spectrum of ANS in the presence of β-lactamase at (A) pH 1.7 and (B) pH 12: (1) no added salt; (2) 0.6 M salt; dotted lines correspond to the spectrum of ANS in the absence of protein. (Reprinted with permission from ref 44. Copyright 1989 American Chemical Society.)

One of the early kinetic studies using ANS was on the folding of the *trp* repressor[45] and revealed that, in the dead-time of the mixing, a significant amount of ANS binds to the protein (compare the intensity at 0 time in Figure 10 to

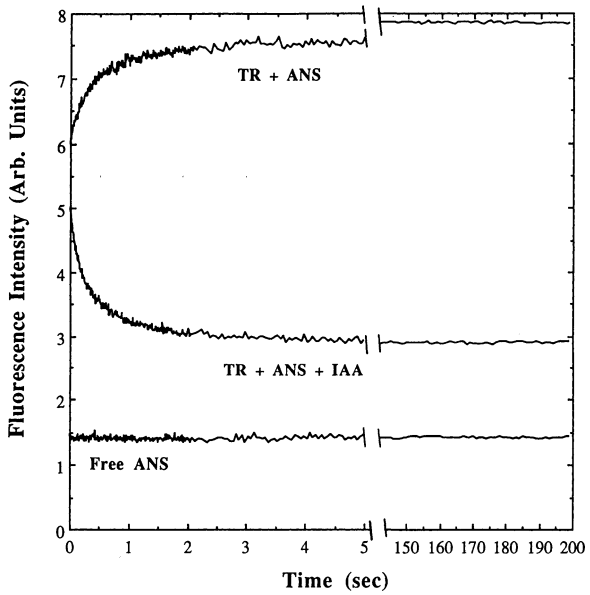

Figure 10. Stopped-flow fluorescence of ANS and the *trp* repressor in a refolding experiment. (Reprinted with permission from ref 45. Copyright 1993 American Chemical Society.)

that of free ANS). However, as was shown subsequently using a comparison of the WT *trp* repressor with a super-repressor mutant AV77, native WT *trp* repressor is not completely folded.[46−48] The valine in place of the alanine at the N-cap position of the D helix stabilizes the helix turn helix domain of the mutant. In the case of WT *trp* repressor, ANS, therefore, binds not only to the early folding intermediate but also to the native apo-protein. Thus, the upper trace in Figure 10 shows not only the burst phase binding to the early intermediate but also an exponential increase in ANS fluorescence as the probe binds to the partially unfolded

tryptophan binding site as the native protein is formed. In the presence of indole acrylic acid, which binds to the tryptophan binding site with high affinity and also orders the structure, like tryptophan, this second exponential phase of increasing fluorescence is not seen. Rather, after the initial burst phase, the ANS intensity actually decreases, indicating that as the fully folded, liganded native state forms, the ANS is ejected from the protein (Figure 10).

This transient binding of ANS is even more evident in the case of dihydrofolate reductase (DHFR),[49] because the native state of this protein does not bind the dye. In Figure 11 is seen an acrylamide quenching study which actually

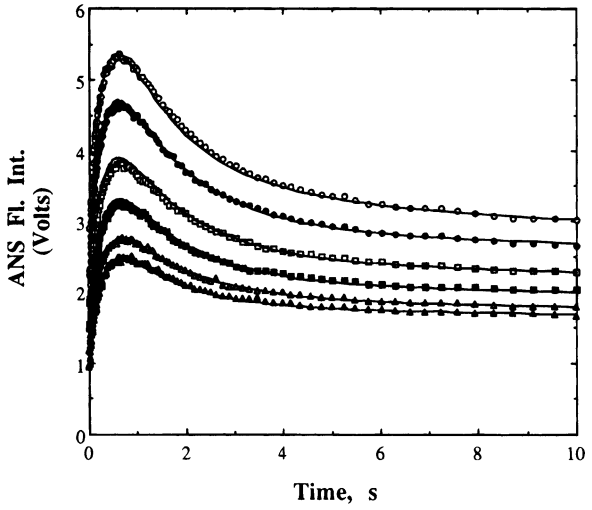

Figure 11. Time-dependence of ANS fluorescence from stopped-flow refolding studies of DHFR as a function of increasing acrylamide concentration (higher acrylamide concentration corresponds to lower intensities). (Reprinted with permission from ref 49. Copyright 1994 American Chemical Society.)

reveals two types of ANS binding sites on the protein, a burst phase site which is highly sensitive to acrylamide concentration, and another site transiently populated on a time scale of hundreds of milliseconds for which the Stern−Volmer quenching constant is significantly smaller. It is also interesting to note that for DHFR (as in most cases) the amplitude of the burst phase ANS intensity decreases in a sigmoidal fashion with increasing denaturant concentration (Figure 12), consistent with the population of an intermediate

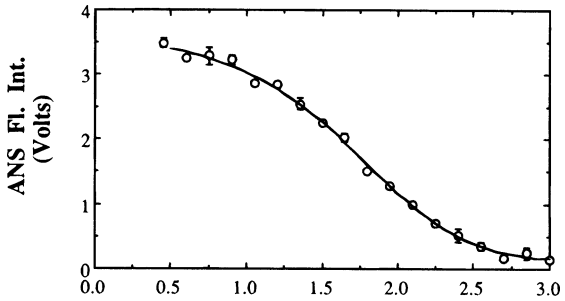

Figure 12. Burst phase intermediate ANS intensity as a function of increasing denaturant. (Reprinted with permission from ref 49. Copyright 1994 American Chemical Society.)

that is destabilized by the denaturant. Thus, although ANS fluorescence does not provide detailed information about the structure of folding intermediates, it presents the advantage of being able to identify them and characterize the kinetics of their population.

3.2. Folding by FRET

Förster resonance energy transfer (FRET) represents one of the few fluorescence-based approaches to protein folding studies that does not report on local structural and dynamic properties but rather provides relatively long-distance information. Because of this property, FRET is particularly useful in characterizing the compaction of the protein chain. FRET is based on the dipolar coupling between the emission dipole of a donor probe and the absorption dipole of an acceptor. With appropriately chosen FRET dye pairs, upon excitation of the donor, FRET results in a quenching of the donor emission and sensitized emission from the acceptor. The probability of this dipolar coupling is dependent upon the sixth power of the distance between the probes (among other things). For the commonly used fluorophores, the distance for 50% transfer, or R_0, is typically around 50−100 Å and depends on the refractive index, n, the relative orientation of the donor and acceptor, κ^2, the quantum yield of the donor, Q_D, and the overlap integral, J, between the emission of the donor and the absorption of the acceptor.

$$R_0 = 0.22(n^{-4}Q_D K^2 J)^{1/6} \quad (1)$$

$$R = R_0\left(\frac{1-\langle E\rangle}{\langle E\rangle}\right)^{1/6} \quad (2)$$

$$\langle E\rangle = 1 - \left(\frac{I_{DA}}{I_D}\right) = 1 - \left(\frac{\tau_{DA}}{\tau_D}\right) \quad (3)$$

Since the FRET efficiency $\langle E\rangle$ measured by the steady-state intensity, I, or fluorescence lifetimes,τ, of the donor only and the donor in the presence of acceptor is such a sensitive indicator of the distance $\langle R\rangle$ between donor and acceptor on a distance scale of tens of angstroms, this technique is very well suited to measuring changes in distances between two positions on objects the size of proteins and protein complexes. For a detailed review of the fundamentals of the FRET technique, see ref 50.

One of the most thorough studies of protein folding using FRET is that by Lillo *et al.* on yeast phosphoglycerate kinase folding (Figure 13).[51,52] It is clear from these in-depth studies that the most difficult and time-consuming aspects of FRET

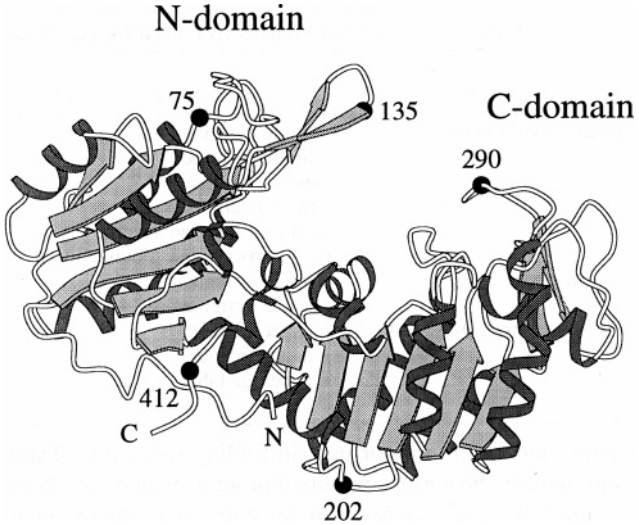

Figure 13. Schematic representation of the structure of yeast PGK (pdb enty 3PGK) showing the position of the residues mutated to cysteine. (Reprinted with permission from ref 51. Copyright 1997 American Chemical Society.)

folding studies are the biochemistry and the data analysis, with the actual FRET experiments being somewhat trivial. To obtain an overall picture of the unfolding of this protein, six double cysteine mutants (and five single cysteine mutants) were constructed and singly or doubly labeled with donor and acceptor. The purified double mutants were labeled individually with a fluorescence donor. These singly donor labeled species were separated from unlabeled and doubly labeled species by anion exchange chromatography. In particular, species singly labeled by donor at position *i* could be separated from species singly labeled by donor at position *j*. The singly labeled double cysteine mutants were then labeled with acceptor on the remaining cysteine and purified from species unreacted with acceptor in the same manner. Singly labeled single and double mutants served as donor only and acceptor only controls in the FRET experiments.

The donor labeling was carried out with IAEDANS, or 5-[[[(2-iodoacetyl)amino]ethyl]amino]naphthalenesulfonic acid), and the acceptor was IAF (iodoacetoamidofluorescein). The R_0 values were calculated using the absorption and emission spectra, the quantum yields, and anisotropy values of the two probes for the six combinations of DA pairs, and they ranged from 42 to 55 Å for the folded structures. Figure 14 shows the distance distributions obtained from the analysis

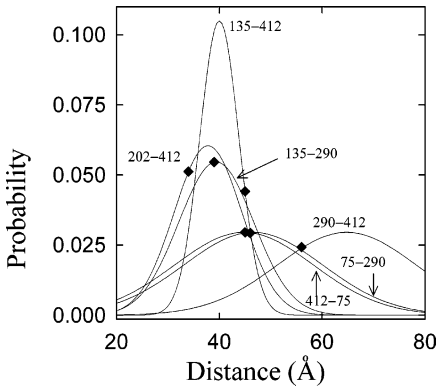

Figure 14. Recovered energy transfer distance distributions from the global analysis of the time-resolved decays of D-PGK and D-PGK-A. The predicted dye-to-dye distances from MD simulations (diamonds) are shown for comparison. (Reprinted with permission from ref 51. Copyright 1997 American Chemical Society.)

of the time-resolved fluorescence intensity decay of the donor only and donor acceptor emissions from the six different FRET pairs.[53] All but the 290−412 pair exhibited distances in agreement with those obtained from molecular dynamics simulations. It was also essential for these studies to ascertain that neither the mutations nor the fluorescent dyes significantly altered the folding properties of the protein. In Figure 15, the overlap of the unfolding profiles from multiple fluorescent observables for the six DA pairs confirms this requirement. In particular, the profile obtained from the decrease in FRET efficiency overlaps that obtained from the intrinsic tryptophan emission for all of the FRET pairs.

These authors went on to carry out stopped-flow kinetics unfolding experiments on all six of the DA pairs (Figure 16).[52] The time-dependent changes in FRET efficiency for each allowed the authors to demonstrate that the unfolding of PGK is a multistep process in which the transition from the native state to the first intermediate involves bending of the hinge between the two domains, such that they separate

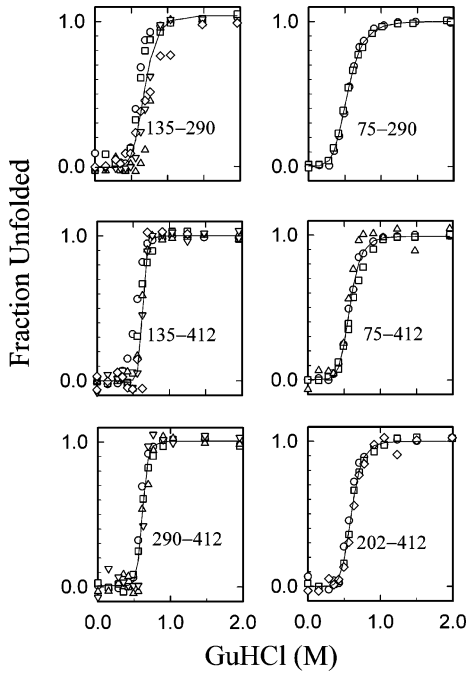

Figure 15. Unfolding of PGK monitored by tryptophan emission from D-PGK and D-PGK-A (circles and squares), AF emission from D-PGK-A (inverted triangles), AEDANS emission from D-PGK (triangles), and FRET efficiency from D-PGK-A (diamonds) for all six FRET pairs. (Reprinted with permission from ref 51. Copyright 1997 American Chemical Society.)

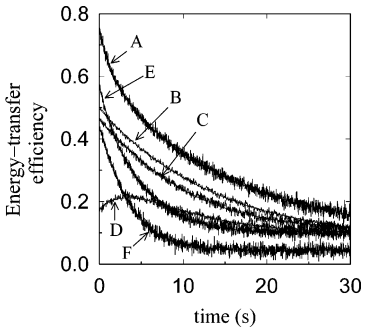

Figure 16. Stopped-flow FRET distances for the six FRET pairs of PGK. (A, 202−412; B, 135−412; C, 412−75; D, 290−412; E, 135−290; F, 75−290). (Reprinted with permission from ref 52. Copyright 1997 American Chemical Society.)

by a distance of about 15 Å. This step is followed by a transition to the I2 intermediate, and finally the unfolded form. Since these studies were published, a number of others have appeared in the literature using FRET to study protein, as well as RNA, folding. Few, however, have provided the level of in-depth verification and care presented in the studies by Lillo and co-workers.

One notable exception is a very complete FRET study on the folding bovine pancreatic Rnase A[54] (Figure 17), in which four tryptophan residues and seven cysteines were inserted by site-directed mutagenesis and the non-native cysteines were labeled with coumarin to create tryptophan to coumarin FRET pairs. This strategy reduces the complexity of the biochemical separations of the donor acceptor pairs since only the single tryptophan and single cysteine mutants are labeled, with only the cysteine being reactive (Figure 17). Figure 18 shows the changes in distance distributions of four of the FRET pairs as a function of increasing concentration of guanidine hydrochloride (GuHCl). These studies allowed the authors to characterize a multistep folding transition and

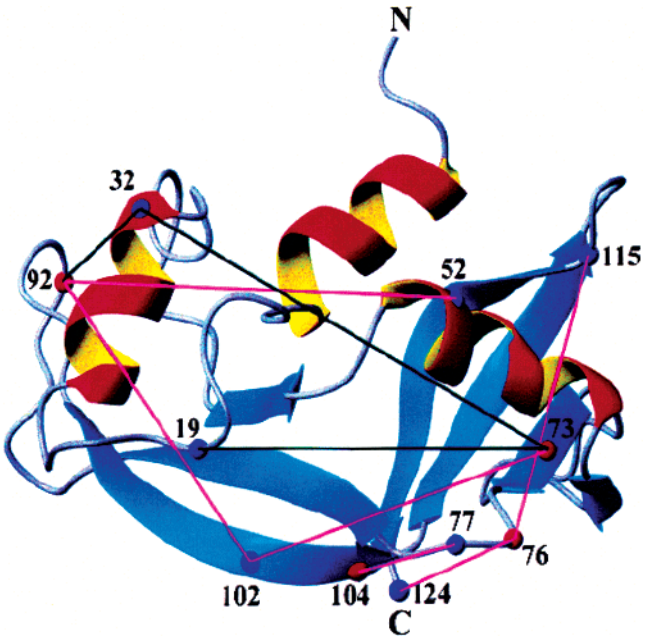

Figure 17. Positions of the four inserted tryptophan residues and the seven inserted cysteine residues in the Rnase A structure. (Reprinted with permission from ref 54. Copyright 2002 American Chemical Society.)

to identify a compact state devoid of any secondary structure yet containing the general structural framework of the folded state. Rapid collapse preceding the rate-limiting step in folding was also evident from FRET-based studies of the folding of cold shock protein.[55] These authors employed tryptophan−AEDANS FRET pairs, placing the AEDANS on cysteine residues engineered onto the surface of this protein. This energy transfer pair with R_0 values near 22 Å was well-suited to the study of the folding of this small protein. Again, the lack of effect of the mutations on the folding parameters was verified.

4. Ultrafast Folding by Fluorescence

How fast can folding be? A recent review suggests that even the ultrafast folding proteins that have been studied to date could be engineered to fold even faster.[56] The high sensitivity and nanosecond time scale of fluorescence make this technique ideal for following the microsecond, and even sub-microsecond, events implicated in folding. As part of their search for the folding speed limit, the Gruebele group set up a laser T-jump apparatus to carry out ultrafast folding experiments by refolding small proteins from a cold denatured state and monitoring the changes in their intrinsic tryptophan fluorescence (e.g., Figure 19).[57,58] Soon after these studies appeared, Thompson and co-workers used a laser temperature-jump apparatus to rapidly unfold a small helical peptide labeled with the extrinsic probe 4-(methylamino)-benzoic acid (MABA) (Figures 20 and 21).[59]

Since these earlier studies using steady-state fluorescence were published, the Greubele group has implemented laser T-jump induced folding coupled with ultrafast acquisition of fluorescence lifetimes[60] (also known as double kinetics experiments) in which one collects nanosecond decay profiles every few microseconds. Recently, this approach has been applied to the study of an extremely fast folding protein,[61] fragment 6−85 of the λ repressor, which exhibited rates under 2 ms, the fasted folding for a protein measured to date. These ultrafast folding experiments based on fluorescence have provided fundamental information about the physical limits of the process. It is important, however, when making these measurements, that one carry out a thorough characterization of the basis for the fluorescence changes that are observed, since the signal-to-noise ratios on these time scales are relatively low.

5. Correlation Spectroscopy and Folding

Single molecule studies represent an approach that should allow examination of the heterogeneity of folding reactions

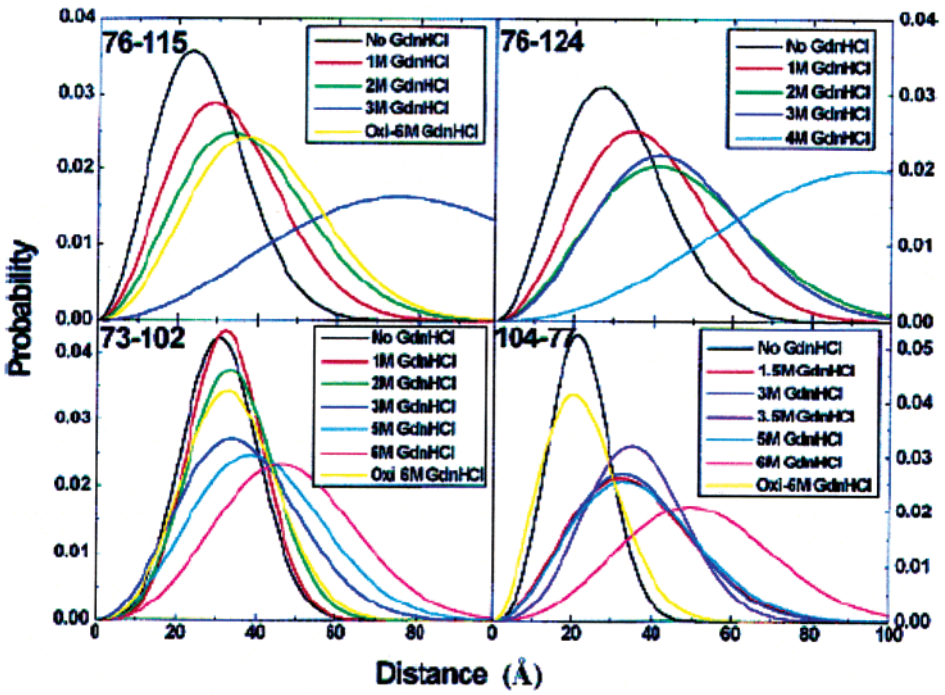

Figure 18. FRET distance distributions at different GuHCl concentrations for doubly labeled RNase A mutants in the reduced native (Rn) and (U) unfolded states. The distances were also determined in the unfolded, oxidized state (Oxi 6M GdnHCl). (Reprinted with permission from ref 54. Copyright 2002 American Chemical Society.)

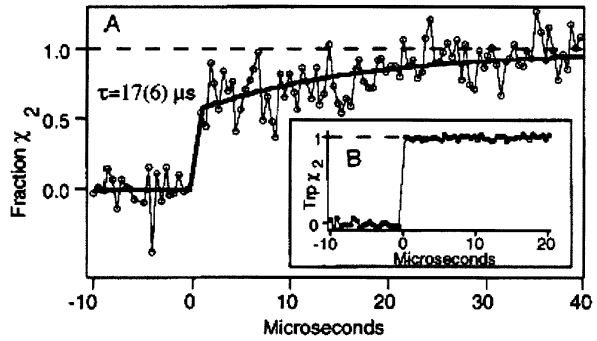

Figure 19. Transient from the folding of horse apomyoglobin after a laser T-jump. The inset (B) shows the response of free tryptophan. (Reprinted with permission from ref 58. Copyright 1993 National Academy of Sciences, U.S.A.)

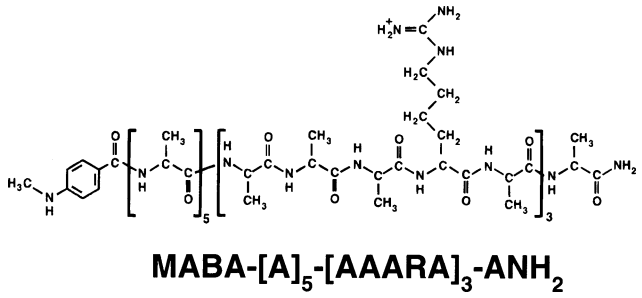

Figure 20. Structure of the helical peptide whose unfolding was followed by rapid laser T-jump. (Reprinted with permission from ref 59. Copyright 1997American Chemical Society.)

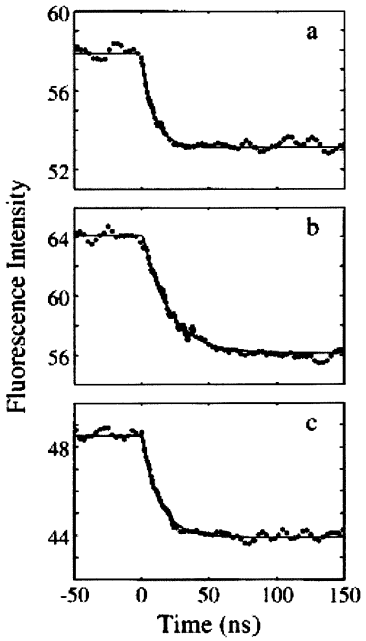

Figure 21. Ultrafast fluorescence intensity kinetic traces after laser T-jumps of (a) 265−275 K, (b) 273−293 K, and 303−319 K. Relaxation times obtained from fits of the data to single exponential decays were on the order of tens of nanoseconds. (Reprinted with permission from ref 59. Copyright 1997 American Chemical Society.)

by comparison of trajectories of multiple single molecules as they fold. Again, given its sensitivity and time scale, fluorescence detection techniques have been largely implemented in these single molecule approaches. In particular, FRET has been used in a number of single molecule folding studies of proteins and RNA.[62−66] Most of the published single molecule folding studies concerning nucleic acids or proteins use histogram and burst analysis of intensity trajectories to characterize the dynamic properties of the system. To follow single molecules over time, they are often, although not always, attached to a surface. However, since single molecule folding is the subject of another review in this series, it will not be covered in the present review. Rather, this review will discuss folding studies using fluctuation spectroscopy, which, although similar to single molecule studies, takes advantage of the time resolution and sensitivity of fluorescence to characterize the dynamic properties of ensembles.

Fluorescence correlation spectroscopy (FCS), which is based on the correlation of the fluctuating intensity signal from the fluorescent dye, allows characterizing conformational dynamics on the microsecond to second time scale, which corresponds to the time scale of protein conformational changes and folding events. Although this approach has not been widely used to date, preliminary results from a number of laboratories, as well as a few published results, suggest that this technique may be quite valuable. To observe protein conformational fluctuations using correlation spectroscopy, one needs to design an experiment such that the conformational change gives rise to a change in the intensity of one or more fluorescent dyes. Analysis of the autocorrelation function, $G(\tau)$, of the fluorescence intensity time traces, $F(t)$, allows for the measure of the time constant of any event that causes the intensity to fluctuate.[67−69] For recent reviews of the FCS technique, see refs 70−72.

For molecules freely diffusing in and out of the small observation volume (either detection using one-photon confocal FCS or excitation using two-photon FCS), fluctuations can be analyzed for the diffusion coefficient, the concentration, and any other process, such as quenching or FRET or photophysical events such as blinking, that cause fluctuations in the observed intensity. The analysis is carried out by calculating the autocorrelation function $G(\tau)$ from the fluctuations of the fluorescence intensity as a function of time $\delta F(t)$.

$$G(\tau) = \frac{\langle \delta F(t) \cdot \delta F(t+\tau) \rangle}{\langle F(t) \rangle^2} \tag{4}$$

In the case where the only fluctuations that are observed arise from uncorrelated noise and the diffusion of the fluorophore in and out of the volume, then the correlation function can be used to determine the translational diffusion time, τ_d.

$$G(\tau) = \left(\frac{1}{V_{\text{eff}} \langle C \rangle}\right)\left(1 + \frac{\tau}{\tau_d}\right)^{-1}\left(1 + \frac{r_0^2 \tau}{z_0^2 \tau_d}\right)^{-1/2} \tag{5}$$

The diffusion time τ_d is inversely proportional to the diffusion coefficient, D,

$$\tau_d = \frac{r_0^2}{4D} \tag{6}$$

where r_0 and z_0 define the effective volume of observation.

$$V_{\text{eff}} = \frac{\pi^{3/2}}{r_0^2 z_0} \tag{7}$$

In the case of additional dynamics resulting in intensity fluctuations,

$$G(\tau) = \chi(\tau)G_D(\tau) \quad (8)$$

$G_D(\tau)$ corresponds to the diffusion part of the correlation function and $\chi(\tau)$ to the dynamics between states A and B

$$\chi(\tau) = (1 - F + Fe^{-t/\tau_F}) \quad (9)$$

In this case τ_F is the relaxation constant,

$$\tau_F = \frac{1}{k_A + k_B} \quad (10)$$

where k_A and k_B are the rate constants of conversion from B to A and A to B, respectively, and F is the fractional population of state A.

$$F = \frac{k_A}{k_A + k_B} \quad (11)$$

The relative values of the relaxation time and the diffusion time determine the extent to which they can be resolved in an FCS experiment. Fluorescence correlation spectroscopy (FCS) studies rely on fluorescence from dye pairs that avoid UV excitation due to the laser sources and microscope optics necessary for these experiments. Typical dye pairs used include Cy3−Cy5, or pairs of Alexa fluorophores (A488−A546 or A488−A568), as well as the more traditional fluorescein−rhodamine pair. R_0 values for these FRET pairs range between 50 and 100 Å, yet in most cases these pairs have been sensitive to the folding transitions, even of rather small proteins and ribozymes.

5.1. Conformational Dynamics

In one of the first studies using FCS to observe conformational dynamics, a cysteine mutant (V60C) of the fatty acid binding protein (FABP) was labeled with fluorescein (V60Flu)[73] (Figure 22). In Figure 23 the improved fit of the autocorrelation function of V60Flu FABP to a model including a 35 μs dynamic intensity fluctuation component in addition to the diffusion coefficient is evidenced by the more random character of the residuals. The amplitude of the conformational fluctuation was found to decrease upon acid unfolding of the protein, consistent with the notion that this fluctuation corresponded to a normal mode of the folded structure. A similar, more recent application uses the cross-correlation between donor and acceptor fluorophores in a FRET experiment on the conformational dynamics of syntaxin 1,[74] fitting in the same manner the cross correlation function for a diffusion and a conformational dynamics component. Interestingly, in these experiments, the observed dynamics around 800 μs were significantly slower than the diffusion. Such behavior has been observed in FCS folding experiments on the small β-barrel protein P13^{MTCP1} (C. Royer, unpublished) and in the calcium-dependent fluctuations in the calmodulin conformation.[75] A recent ultrafast FCS study of the small trp cage protein by tryptophan quenching of a covalently bound extrinsic dye revealed a collapsed intermediate under native conditions.[99] As for all fluorescence observables, one must use caution in interpreting these changes, and it is particularly important to carry out all the more classical fluorescence approaches in order to thoroughly characterize the changes that are observed. Assigning fluorescence intensity fluctuations to particular dynamic modes in proteins should be done with the utmost caution.

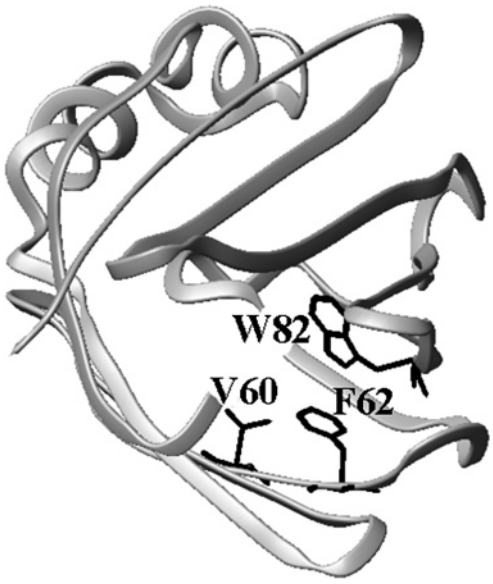

Figure 22. Crystal structure of the FABP showing the position of the V60C mutation and the two fluorophores likely responsible for the quenching of the fluorescein label at position 60. (Reprinted with permission from ref 73. Copyright 2002 National Academy of Sciences, U.S.A.)

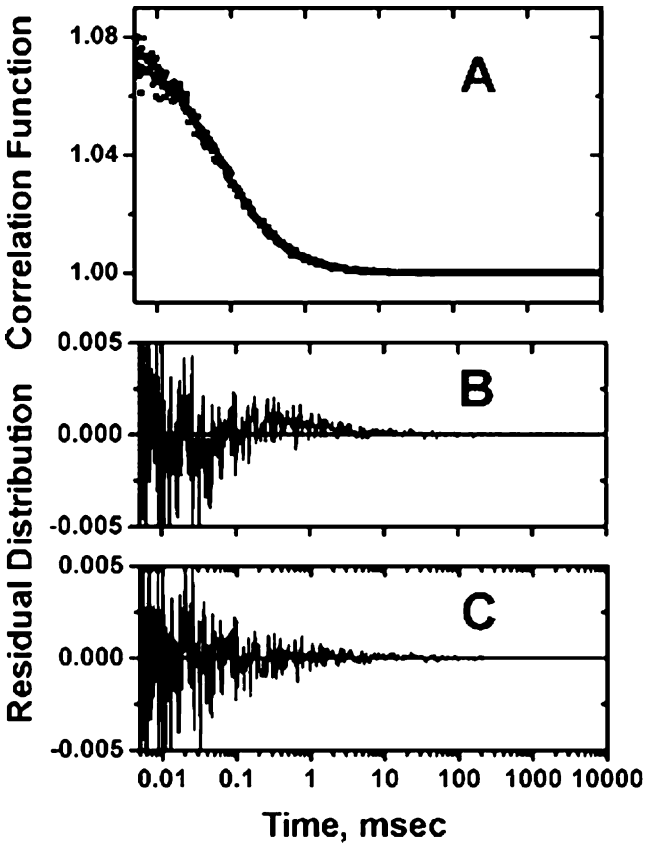

Figure 23. Autocorrelation function and residuals of the simple diffusion model and an additional dynamics model for V60Flu FABP. (Reprinted with permission from ref 73. Copyright 2002 National Academy of Sciences, U.S.A.)

5.2. FCS, Folding, and Aggregation

One of the major goals in the field of protein folding is elucidating the factors that control the process of folding vs

aggregation. Indeed, amyloid diseases (about 20 are known to date, such as Alzheimer's disease, Parkinson's disease, type II diabetes, and bovine spongiform encephalitis) involve the accumulation of specific protein aggregates in various organs and tissues.[76] Contrary to the well-known differences in the three-dimensional structures of the native forms of these proteins, their aggregation leads to the formation of very similar fibers exhibiting cross β X-ray diffraction patterns characteristic of structures containing β-sheets whose axes run perpendicular to the fibril axis. While each disease involves a specific protein aggregate, it appears from *in vitro* studies that any protein, under appropriate conditions, can undergo the structural transition to amyloid fibers.[77] Key to the transition is exposing hydrophobic surfaces to solvent by forcing the population of partially folded intermediates, either by placing the protein under specific solvent conditions, by limited proteolysis, or by site specific mutations. Amyloid diseases are often hereditary because certain mutations favor the aggregation process over folding. The process of forming the amyloid fibers generally exhibits a lag phase, which can be shortened by the addition of preformed aggregates, followed by a phase of rapid growth. Amyloidogenesis apparently proceeds by the formation of soluble oligomers, followed by their assembly into prefibrillar aggregates (some annular, some beadlike), then protofibrils, and finally mature amyloid fibers. It is not clear which species are predominant during the lag phase and more importantly which are responsible for the various pathologies.

FCS is particularly well-suited to the characterization of protein oligomers and aggregates. For example, in fluorescence anisotropy measurements which allow for the determination of the rotational diffusion coefficient of the labeled molecules, the size of the observable oligomers is limited by the lifetime of the fluorophore. Typical dyes exhibit lifetimes on the order of a few nanoseconds, such that rotational correlation time values greater than 50 ns (corresponding to a globular protein of 125 kDa) are generally beyond the limits of the technique. On the other hand, the size of the oligomers observable by FCS is not limited by the fluorescence lifetime. Thus, although the translational diffusion coefficient measured by FCS increases only with the cube root of the molecular weight, rather than linearly as in the case of rotational diffusion measurements, for large aggregates, FCS is much more sensitive. Compared to analytical ultracentrifugation, which also is based on translational diffusion, FCS is much faster and requires considerably less material. Since FCS measurements can be made in a few seconds, and in flow devices, the kinetics of aggregation can be assessed. Finally, FCS measurements can be made inside living cells.[78] As seen in Figure 24, rather than simply providing a global view of the aggregation process, the diffusion curves can be analyzed in terms of several discreet diffusing species.[79] Such measurements can be quite useful in characterizing the transitions from soluble oligomers, to prefibrillar aggregates, to fibers.[79,80] Again, since these measurements can be made *in vivo*, one may be able to follow formation of amyloid fibers in the cellular environment. Such an approach could also be extended to the study of viral assembly.

6. Folding in Vivo Using Fluorescence

Much progress has been made in the last 10 or 15 years in defining the factors that control protein folding and stability. The protein folding reaction and energy landscape are reasonably well-understood, on both an experimental and theoretical level. Our ability to predict protein structure, not only by homology modeling but also *ab initio*, has progressed considerably, as well. The next step, from understanding folding to understanding the links between folding and function, has been undertaken. Despite this undeniable progress, characterizing protein folding and stability *in vivo* remains a key challenge to the folding field. As has been the case in the past for *in vitro* studies of protein folding, fluorescence will undoubtedly play a major role in future investigations of the fate of proteins in the cell. Indeed, fluorescence microscopy represents the principle method of observation of cellular processes. The advent and constant innovation of new tools such as laser-scanning confocal and two-photon microscopy, FCS *in vivo*, and single particle tracking and the development and refinement of new fluorescent probes including the fluorescent proteins,[81,82] FlaSH and ReASH[83] dyes, and quantum dots[84,85] hold enormous promise for the future of the application of fluorescence methodologies to characterizing protein folding and stability *in vivo*.

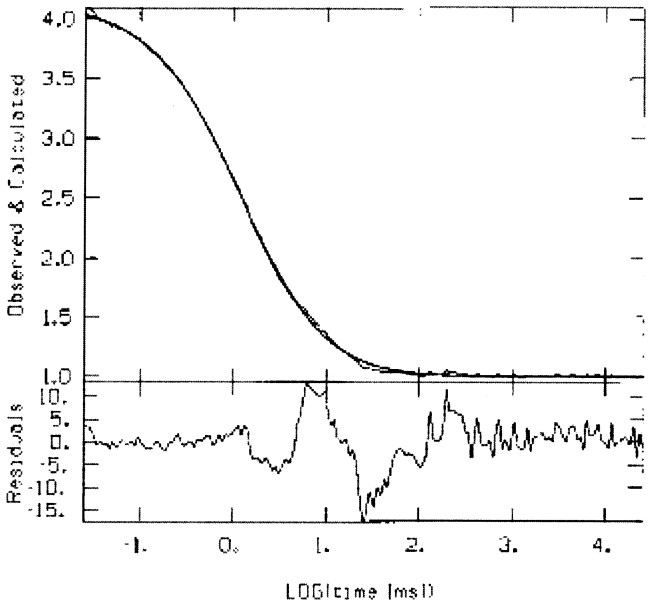

Figure 24. Autocorrelation of Cy5 labeled fibrinogen after activation with thrombin. Analysis yielded diffusion times of 0.11, 0.97, and 2.4 ms. (Reprinted with permission from ref 79. Copyright 1999 Elsevier.)

While the study of protein folding *in vitro* certainly has presented its fair share of challenges and technical and theoretical difficulties, tackling the protein folding problem *in vivo* (taken here to refer to studies in live cells) presents a far more complex set of issues. As for the situation *in vitro*, protein folding *in vivo* implicates the primary sequence of the protein, coupling or uncoupling of domain folding, coupled folding and assembly of protein oligomers, and competing aggregation reactions. Moreover, in addition to these complications, folding *in vivo* implicates a number of other processes and biomolecular partners such as coupled translation and folding, the intervention of chaperones, translocation, export and targeting machinery, proteasomes, and degradation signals. Taken together, these complexities can make the idea of studying protein folding *in vivo* appear a daunting task indeed.[86,87] This complexity not withstanding, significant advances have been made recently in characterizing the folding phenomenon within the cell. These advances

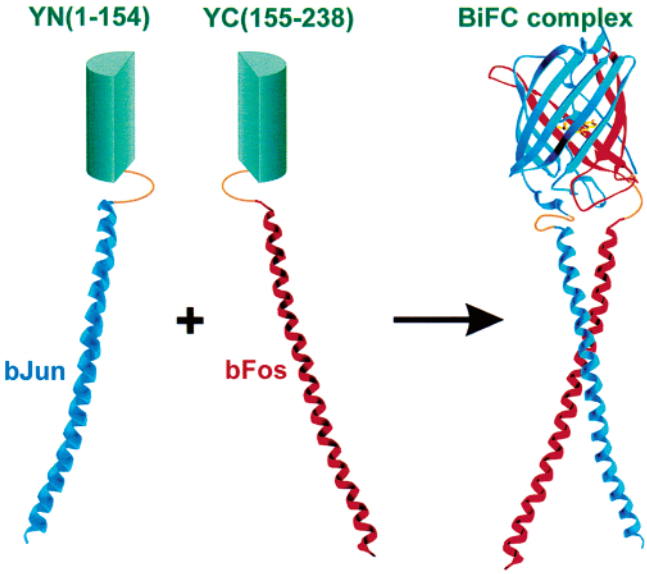

Figure 25. Schematic description of the YFP-fragment-based assay showing the two halves of the fluorescent protein fused respectively to one or the other leucine-zipper transcription factor. (Reprinted with permission from ref 88. Copyright 2002 Elsevier.)

have generally been based on studies using, among other approaches, fluorescence-based techniques.

A clever scheme for monitoring protein association *in vivo* was developed by Kerppola and co-workers.[88] These investigators took advantage of the fact that the maturation of the fluorophore in the naturally fluorescent proteins (GFP, YFP, etc.) only occurs after folding and that the mixing of the N-terminal and C-terminal halves of these proteins leads to folding and generation of the fluorophore. Coexpression of fusion proteins of heterodimers, with one partner fused to the C-terminal half of the yellow fluorescent protein and the other heterodimer partner fused to the N-terminal half, results in strong fluorescence upon interaction of the two partners in the cell (Figure 25). In Figure 26 the coexpression in Cos-1

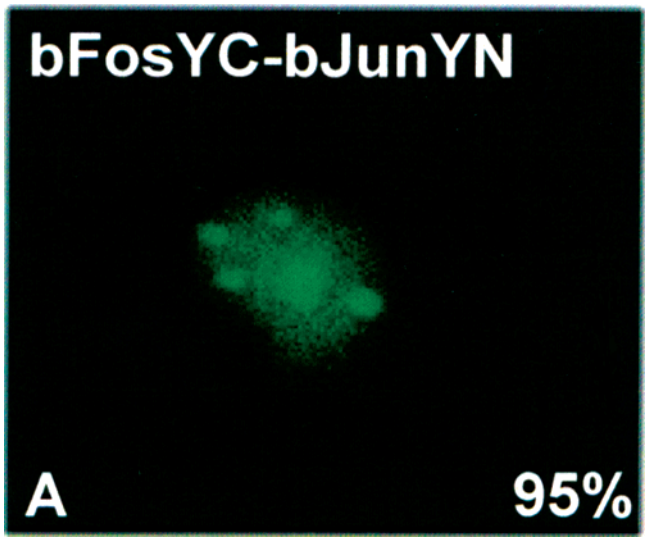

Figure 26. Fluorescence image of a Cos-1 cell expressing p50 and p65 fusions with the N- and C-terminal halves of YFP, respectively. (Reprinted with permission from ref 88. Copyright 2002 Elsevier.)

cells of the APl heterodimers, bJun fused to the N-terminal half of YFP and bFos fused to the C-terminal half, results in strong fluorescence. A FRET assay for protein folding *in*

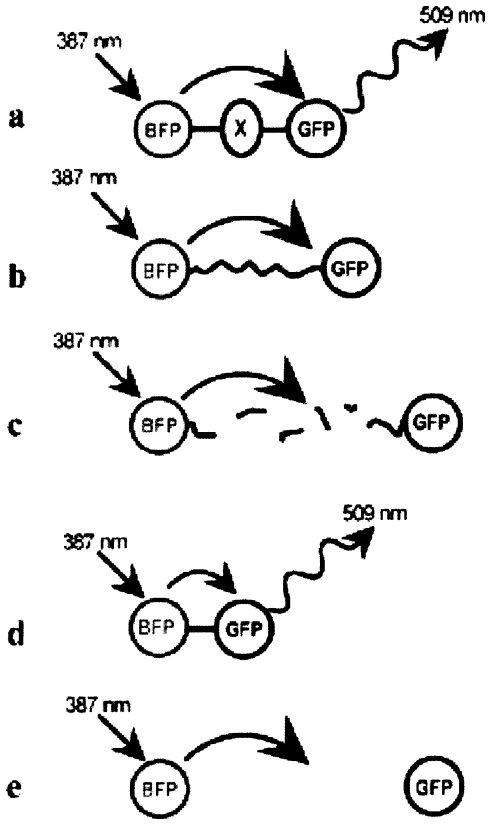

Figure 27. Schematic description of the *in vivo* FRET-based assay for protein folding using the naturally fluorescent proteins BFP and GFP. FRET only occurs when the protein is in the folded state. (Reprinted with permission from ref 89. Copyright 2003 Elsevier.)

vivo has also been developed[89] (Figure 27). In this assay the gene for the fluorescent protein donor (BFP) is fused on the 5′end of the coding sequence for the protein of interest and the gene for the fluorescent protein acceptor (GFP) is fused onto the 3′-end. Efficient FRET only occurs if the protein is folded. It is interesting to note that cross-correlation

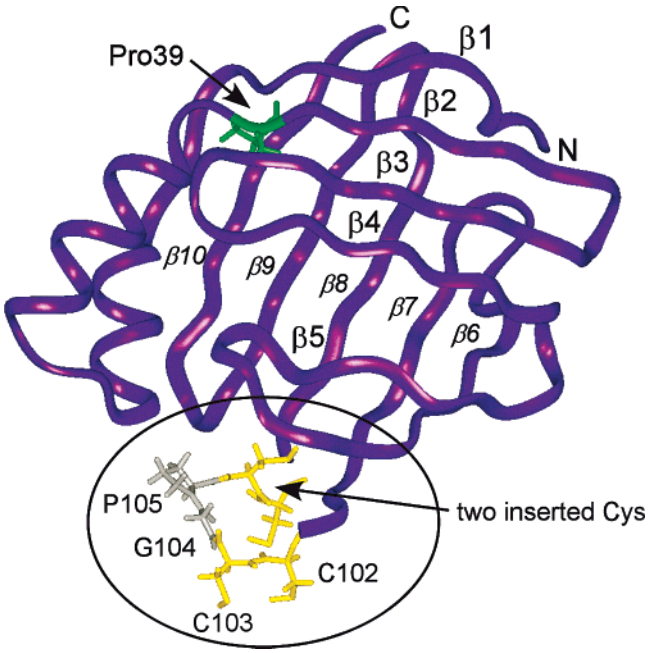

Figure 28. Ribbon diagram of CRABP I showing a model of the inserted FlaSH binding site. (Reprinted with permission from ref 90. Copyright 2004 National Academy of Sciences, U.S.A.)

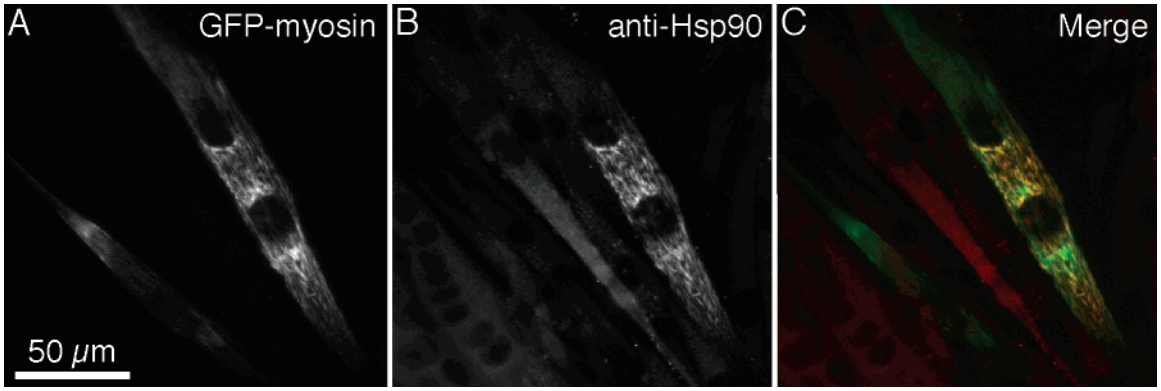

Figure 29. Immunofluorescence microscopy of C2C12 cells expressing GFP-myosin (green channel, A) and Hsp90 antibody (red channel, B) after fixation and staining. (Reprinted with permission from ref 91. Copyright 2004 The Company of Biologists Ltd.)

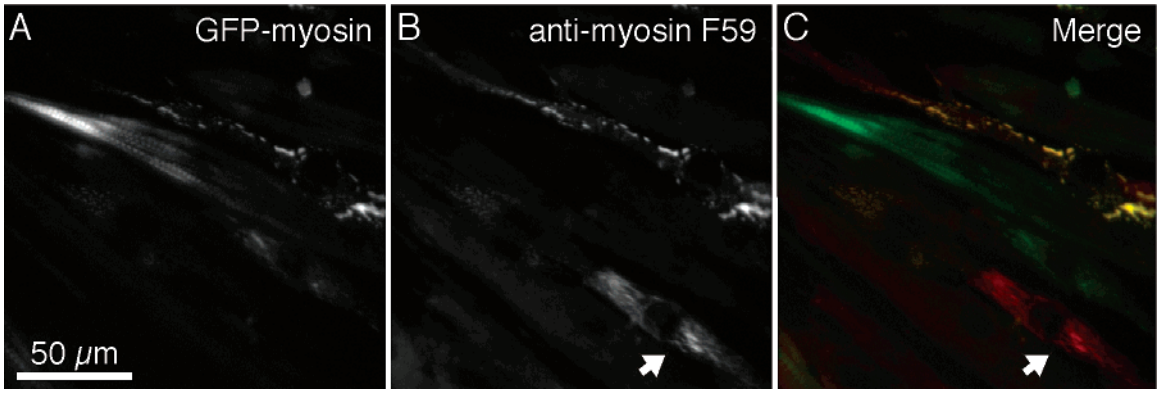

Figure 30. In paraformaldehyde fixed C2C12 cells the GFP-myosin is found in striated myofibrils and in folding intermediates (A). The F59 antibody labels the intermediates (B), not the folded myofibrils (C). (Reprinted with permission from ref 91. Copyright 2004 The Company of Biologists Ltd.)

studies by two-photon FCS could be used to distinguish between unfolded protein and proteolysis because the FRET in both cases (unfolded and proteolyzed protein) would be low but the cross-correlation signal would only be significant in the case of the unfolded protein, whereas in the case of the cleaved products no cross-correlation should be observed. Finally, a screen based on the enhancement of the fluorescence intensity of the FlaSH dye for which a site was engineered into a turn of the mammalian cellular retinoic acid binding protein I (CRABP I)[90] (Figure 28) showed that the cooperativity of urea-induced unfolding was higher *in vivo* and that large scale aggregation could be detected *in vivo* with an aggregation prone mutant.

In addition to these screens to monitor the folding of test proteins *in vivo*, studies have been carried out that have probed the folding, stability, and fate of particular proteins in their physiologically relevant environments. For example, using myosin fused to GFP, in combination with fluorescently labeled antibodies against partially folded forms of the protein and against the heat shock protein Hsp90, Srikakulam and Winkelmann[91] were able to detect intermediates in myosin folding *in vivo*. They showed that in the early stages of muscle differentiation, GFP−myosin accumulates in bright globular foci and short filamentous structures that also contain Hsp90 (Figure 29) and Hsc70, and that these structures also stain with conformationally sensitive antibodies that recognize the unfolded conformation of the motor domain and the coiled coil conformation of the rod (Figure 30).

A number of other studies using fluorescent proteins have appeared recently that report on the fate of proteins in cells. These include a report on the interactions of rhodopsin with chaperones,[92] another on the coupled folding and binding of the bacterial integration host factor subunits α and *β*,[93] a study on the translocation of proteins by the bacterial Tat system,[94] and one of protein degradation by the Clp Hsp100 ATPases.[95] These examples demonstrate that much can be, and surely will be, learned about protein folding i*n vivo* as more tools become available. The challenge now is to push the limits of our capabilities in order to make more detailed, direct measurements of biophysical properties in cells. As the molecular players in these processes continue to be identified, biophysicists should concentrate on characterizing their interactions and the dynamics of these assemblies in the cell.

7. Conclusions

It is interesting to reflect upon the perceived popularity of certain techniques, such as fluorescence, and how this perception may change with time. In the early to mid 1990s, fluorescence was considered by many to be an old technique, not worth a great deal of resources and effort. Nonetheless, it continued to be used in classical fashion, as well as truly innovative ways, as can be seen from the reading of the papers cited in this review. Over the past few years, fluorescence has gained in popularity, as many of the new approaches have become more widely known and appreciated. Despite these variations in the level of appreciation, it is important to bear in mind that the appropriate use of a biophysical method (whatever it may be) requires the existence of a field of study made up of generations of

researchers who over time work together, argue over approaches and results, and discuss new ideas and possibilities. Whether the current trend for a technique is to use it regardless of the circumstances or rather to decry its lack of applicability, it is important to try to resist these trends and to continue to carry out careful, yet state of the art experiments, always pushing the limits of the technique in question.

This said, given their many advantages, fluorescence approaches will no doubt continue to be applied in the fields of biophysics and biophysical chemistry for a very long time. Although fluorescence does not provide detailed structural information, its utility in defining structural dynamics and molecular interactions place it at the top of the possible methods that could be applied in addressing such questions. Clearly, fluorescence, like any technique, should not be used alone. Rather, its lack of capabilities on the structural level should be compensated for by the use of complementary approaches.

8. References

(1) Matouschek, A.; Kellis, J. T., Jr.; Serrano, L.; Fersht, A. R. *Nature* **1989**, *340*, 122.
(2) Serrano, L.; Kellis, J. T., Jr.; Cann, P.; Matouschek, A.; Fersht, A. R. *J. Mol. Biol.* **1992**, *224*, 783.
(3) Serrano, L.; Matouschek, A.; Fersht, A. R. *J. Mol. Biol.* **1992**, *224*, 805.
(4) Serrano, L.; Matouschek, A.; Fersht, A. R. *J. Mol. Biol.* **1992**, *224*, 847.
(5) Matouschek, A.; Serrano, L.; Fersht, A. R. *J. Mol. Biol.* **1992**, *224*, 819.
(6) Fersht, A. R.; Matouschek, A.; Serrano, L. *J. Mol. Biol.* **1992**, *224*, 771.
(7) Pierce, D. W.; Boxer, S. G. *Biophys. J.* **1995**, *68*, 1583.
(8) Szabo, A. G.; Stepanik, T. M.; Wayner, D. M.; Young, N. M. *Biophys. J.* **1983**, *41*, 233.
(9) Royer, C. A.; Hinck, A. P.; Loh, S. N.; Prehoda, K. E.; Peng, X.; Jonas, J.; Markley, J. L. *Biochemistry* **1993**, *32*, 5222.
(10) Declerck, N.; Dutartre, H.; Receveur, V.; Dubois, V.; Royer, C.; Aymerich, S.; van, T. H. *J. Mol. Biol.* **2001**, *314*, 671.
(11) Adams, P. D.; Chen, Y.; Ma, K.; Zagorski, M. G.; Sonnichsen, F. D.; McLaughlin, M. L.; Barkley, M. D. *J. Am. Chem. Soc.* **2002**, *124*, 9278.
(12) Chen, Y.; Barkley, M. D. *Biochemistry* **1998**, *37*, 9976.
(13) Chen, R. F.; Knutson, J. R.; Ziffer, H.; Porter, D. *Biochemistry* **1991**, *30*, 5184.
(14) Laws, W. R.; Ross, J. B.; Wyssbrod, H. R.; Beechem, J. M.; Brand, L.; Sutherland, J. C. *Biochemistry* **1986**, *25*, 599.
(15) Ross, J. B.; Wyssbrod, H. R.; Porter, R. A.; Schwartz, G. P.; Michaels, C. A.; Laws, W. R. *Biochemistry* **1992**, *31*, 1585.
(16) Willis, K. J.; Neugebauer, W.; Sikorska, M.; Szabo, A. G. *Biophys. J.* **1994**, *66*, 1623.
(17) Roumestand, C.; Boyer, M.; Guignard, L.; Barthe, P.; Royer, C. A. *J. Mol. Biol.* **2001**, *312*, 247.
(18) Royer, C. A.; Mann, C. J.; Matthews, C. R. *Protein Sci.* **1993**, *2*, 1844.
(19) Vidugiris, G. J.; Markley, J. L.; Royer, C. A. *Biochemistry* **1995**, *34*, 4909.
(20) Scalley, M. L.; Yi, Q.; Gu, H.; McCormack, A.; Yates, J. R., III; Baker, D. *Biochemistry* **1997**, *36*, 3373.
(21) Yi, Q.; Scalley, M. L.; Simons, K. T.; Gladwin, S. T.; Baker, D. *Folding Des.* **1997**, *2*, 271.
(22) Gu, H.; Kim, D.; Baker, D. *J. Mol. Biol.* **1997**, *274*, 588.
(23) Kim, D. E.; Yi, Q.; Gladwin, S. T.; Goldberg, J. M.; Baker, D. *J. Mol. Biol.* **1998**, *284*, 807.
(24) Plaxco, K. W.; Baker, D. *Proc. Natl. Acad. Sci. U.S.A.* **1998**, *95*, 13591.
(25) Plaxco, K. W.; Millett, I. S.; Segel, D. J.; Doniach, S.; Baker, D. *Nat. Struct. Biol.* **1999**, *6*, 554.
(26) Kim, D. E.; Fisher, C.; Baker, D. *J. Mol. Biol.* **2000**, *298*, 971.
(27) Hannemann, F.; Bera, A. K.; Fischer, B.; Lisurek, M.; Teuchner, K.; Bernhardt, R. *Biochemistry* **2002**, *41*, 11008.
(28) Epstein, H. F.; Schechter, A. N.; Chen, R. F.; Anfinsen, C. B. *J. Mol. Biol.* **1971**, *60*, 499.
(29) Hynes, T. R.; Fox, R. O. *Proteins* **1991**, *10*, 92.
(30) Yin, J.; Jing, G. *J. Biochem. (Tokyo)* **2000**, *128*, 113.
(31) Flanagan, J. M.; Kataoka, M.; Shortle, D.; Engelman, D. M. *Proc. Natl. Acad. Sci. U.S.A.* **1992**, *89*, 748.
(32) Otto, M. R.; Lillo, M. P.; Beechem, J. M. *Biophys. J.* **1994**, *67*, 2511.
(33) Maki, K.; Cheng, H.; Dolgikh, D. A.; Shastry, M. C.; Roder, H. *J. Mol. Biol.* **2004**, *338*, 383.
(34) Beechem, J. M. *Methods Enzymol.* **1992**, *210*, 37.
(35) Knutson, J. R.; Walbridge, D. G.; Brand, L. *Biochemistry* **1982**, *21*, 4671.
(36) Mann, C. J.; Royer, C. A.; Matthews, C. R. *Protein Sci.* **1993**, *2*, 1853.
(37) Fernando, T.; Royer, C. A. *Biochemistry* **1992**, *31*, 6683.
(38) Vangala, S.; Vidugiris, G. A. J.; Royer, C. A. *J. Fluoresc.* **1998**, *8* (1), 1.
(39) Ross, J. B.; Laws, W. R.; Sutherland, J. C.; Buku, A.; Katsoyannis, P. G.; Schwartz, I. L.; Wyssbrod, H. R. *Photochem. Photobiol.* **1986**, *44*, 365.
(40) Weber, G.; Laurence, D. J. *Process Biochem.* **1954**, *56*, xxxi.
(41) Weber, G.; Young, L. B. *J. Biol. Chem.* **1964**, *239*, 1415.
(42) Stryer, L. *J. Mol. Biol.* **1965**, *13*, 482.
(43) Turner, D. C.; Brand, L. *Biochemistry* **1968**, *7*, 3381.
(44) Goto, Y.; Fink, A. L. *Biochemistry* **1989**, *28*, 945.
(45) Mann, C. J.; Matthews, C. R. *Biochemistry* **1993**, *32*, 5282.
(46) Reedstrom, R. J.; Royer, C. A. *J. Mol. Biol.* **1995**, *253*, 266.
(47) Spolar, R. S.; Record, M. T., Jr. *Science* **1994**, *263*, 777.
(48) Gryk, M. R.; Jardetzky, O. *J. Mol. Biol.* **1996**, *255*, 204.
(49) Jones, B. E.; Jennings, P. A.; Pierre, R. A.; Matthews, C. R. *Biochemistry* **1994**, *33*, 15250.
(50) Clegg, R. M. *Curr. Opin. Biotechnol.* **1995**, *6*, 103.
(51) Lillo, M. P.; Beechem, J. M.; Szpikowska, B. K.; Sherman, M. A.; Mas, M. T. *Biochemistry* **1997**, *36*, 11261.
(52) Lillo, M. P.; Szpikowska, B. K.; Mas, M. T.; Sutin, J. D.; Beechem, J. M. *Biochemistry* **1997**, *36*, 11273.
(53) Beechem, J. M. *Chem. Phys. Lipids* **1989**, *50*, 237.
(54) Navon, A.; Ittah, V.; Scheraga, H. A.; Haas, E. *Biochemistry* **2002**, *41*, 14225.
(55) Magg, C.; Schmid, F. X. *J. Mol. Biol.* **2004**, *335*, 1309.
(56) Kubelka, J.; Hofrichter, J.; Eaton, W. A. *Curr. Opin. Struct. Biol.* **2004**, *14*, 76.
(57) Ballew, R. M.; Sabelko, J.; Gruebele, M. *Nat. Struct. Biol.* **1996**, *3*, 923.
(58) Ballew, R. M.; Sabelko, J.; Gruebele, M. *Proc. Natl. Acad. Sci. U.S.A.* **1996**, *93*, 5759.
(59) Thompson, P. A.; Eaton, W. A.; Hofrichter, J. *Biochemistry* **1997**, *36*, 9200.
(60) Ervin, J.; Sabelko, J.; Gruebele, M. *J. Photochem. Photobiol. B* **2000**, *54*, 1.
(61) Yang, W. Y.; Gruebele, M. *Biophys. J.* **2004**, *87*, 596.
(62) Lipman, E. A.; Schuler, B.; Bakajin, O.; Eaton, W. A. *Science* **2003**, *301*, 1233.
(63) Schuler, B.; Lipman, E. A.; Eaton, W. A. *Nature* **2002**, *419*, 743.
(64) Deniz, A. A.; Laurence, T. A.; Beligere, G. S.; Dahan, M.; Martin, A. B.; Chemla, D. S.; Dawson, P. E.; Schultz, P. G.; Weiss, S. *Proc. Natl. Acad. Sci. U.S.A.* **2000**, *97*, 5179.
(65) Zhuang, X.; Kim, H.; Pereira, M. J.; Babcock, H. P.; Walter, N. G.; Chu, S. *Science* **2002**, *296*, 1473.
(66) Zhuang, X.; Bartley, L. E.; Babcock, H. P.; Russell, R.; Ha, T.; Herschlag, D.; Chu, S. *Science* **2000**, *288*, 2048.
(67) Elson, E. L.; Schlessinger, J.; Koppel, D. E.; Axelrod, D.; Webb, W. W. *Prog. Clin. Biol. Res.* **1976**, *9*, 137.
(68) Elson, E. L.; Webb, W. W. *Annu. Rev. Biophys. Bioeng.* **1975**, *4*, 311.
(69) Magde, D.; Elson, E. L.; Webb, W. W. *Biopolymers* **1974**, *13*, 29.
(70) Bacia, K.; Schwille, P. *Methods* **2003**, *29*, 74.
(71) Haustein, E.; Schwille, P. *Methods* **2003**, *29*, 153.
(72) Medina, M. A.; Schwille, P. *Bioessays* **2002**, *24*, 758.
(73) Chattopadhyay, K.; Saffarian, S.; Elson, E. L.; Frieden, C. *Proc. Natl. Acad. Sci. U.S.A.* **2002**, *99*, 14171.
(74) Margittai, M.; Widengren, J.; Schweinberger, E.; Schroder, G. F.; Felekyan, S.; Haustein, E.; Konig, M.; Fasshauer, D.; Grubmuller, H.; Jahn, R.; Seidel, C. A. *Proc. Natl. Acad. Sci. U.S.A.* **2003**, *100*, 15516.
(75) Slaughter, B. D.; Allen, M. W.; Unruh, J. R.; Bieber, R. J.; Johnson, C. K. *J. Phys. Chem. B* **2004**, *108*, 10388.
(76) Dobson, C. M. *Nature* **2003**, *426*, 884.
(77) Dobson, C. M. *Trends Biochem. Sci.* **1999**, *24*, 329.
(78) Kim, S. A.; Heinze, K. G.; Waxham, M. N.; Schwille, P. *Proc. Natl. Acad. Sci. U.S.A.* **2004**, *101*, 105.
(79) Bark, N.; Foldes-Papp, Z.; Rigler, R. *Biochem. Biophys. Res. Commun.* **1999**, *260*, 35.
(80) Tjernberg, L. O.; Pramanik, A.; Bjorling, S.; Thyberg, P.; Thyberg, J.; Nordstedt, C.; Berndt, K. D.; Terenius, L.; Rigler, R. *Chem. Biol.* **1999**, *6*, 53.
(81) Scarlata, S.; Dowal, L. *Methods Mol. Biol.* **2004**, *237*, 223.

(82) Lippincott-Schwartz, J.; Patterson, G. H. *Science* **2003**, *300*, 87.
(83) Adams, S. R.; Campbell, R. E.; Gross, L. A.; Martin, B. R.; Walkup, G. K.; Yao, Y.; Llopis, J.; Tsien, R. Y. *J. Am. Chem. Soc.* **2002**, *124*, 6063.
(84) Gao, X.; Nie, S. *Trends Biotechnol.* **2003**, *21*, 371.
(85) Chan, W. C.; Maxwell, D. J.; Gao, X.; Bailey, R. E.; Han, M.; Nie, S. *Curr. Opin. Biotechnol.* **2002**, *13*, 40.
(86) Imai, J.; Yashiroda, H.; Maruya, M.; Yahara, I.; Tanaka, K. *Cell Cycle* **2003**, *2*, 585.
(87) Bross, P.; Gregersen, N. *Methods Mol. Biol.* **2003**, *232*, 17.
(88) Hu, C. D.; Chinenov, Y.; Kerppola, T. K. *Mol. Cell* **2002**, *9*, 789.
(89) Philipps, B.; Hennecke, J.; Glockshuber, R. *J. Mol. Biol.* **2003**, *327*, 239.
(90) Ignatova, Z.; Gierasch, L. M. *Proc. Natl. Acad. Sci. U.S.A.* **2004**, *101*, 523.
(91) Srikakulam, R.; Winkelmann, D. A. *J. Cell Sci.* **2004**, *117*, 641.
(92) Chapple, J. P.; Cheetham, M. E. *J. Biol. Chem.* **2003**, *278*, 19087.
(93) Wang, H.; Chong, S. *Proc. Natl. Acad. Sci. U.S.A.* **2003**, *100*, 478.
(94) Ize, B.; Gerard, F.; Zhang, M.; Chanal, A.; Voulhoux, R.; Palmer, T.; Filloux, A.; Wu, L. F. *J. Mol. Biol.* **2002**, *317*, 327.
(95) Hoskins, J. R.; Yanagihara, K.; Mizuuchi, K.; Wickner, S. *Proc. Natl. Acad. Sci. U.S.A.* **2002**, *99*, 11037.
(96) O'Neill, J. W.; Kim, D. E.; Baker, D.; Zhang, K. Y. *Acta Crystallogr., D: Biol. Crystallogr.* **2001**, *57*, 480.
(97) Royer, C. A.; Hinck, A. P.; Loh, S. N.; Prehoda, K. E.; Peng, X.; Jonas, J.; Markley, J. L. *Biochemistry* **1993**, *32*, 5222.
(98) Zhang, R. G.; Joachimiak, A.; Lawson, C. L.; Schevitz, R. W.; Otwinowski, Z.; Sigler, P. B. *Nature* **1987**, *327*, 591.
(99) Neuweiler, H.; Doose, S.; Sauer, M. *Proc. Natl. Acad. Sci. U.S.A.* **2005**, *102*, 16650−16655.

CR0404390